

1 **Functional connectivity directionality between large-scale resting-state networks in**
2 **children and adolescence from the Healthy Brain Network sample**

3
4 Martina J. Lund^{1*}, Dag Alnæs^{1,2}, Jaroslav Rokicki^{1,3}, Simon Schwab^{4,5}, Ole A. Andreassen^{1,6},
5 Lars T. Westlye^{1,3,6}, Tobias Kaufmann^{1,7*}.

6
7 ¹ Norwegian Centre for Mental Disorders Research (NORMENT), Division of Mental Health
8 and Addiction, Oslo University Hospital, and Institute of Clinical Medicine, University of
9 Oslo, Norway

10 ² Bjørknes College, Oslo, Norway

11 ³ Department of Psychology, University of Oslo, Oslo, Norway

12 ⁴ Center for Reproducible Science (CRS) & Epidemiology, Biostatistics and Prevention
13 Institute (EBPI), University of Zurich, Zurich, Switzerland

14 ⁵ Big Data Institute, Li Ka Shing Centre for Health Information and Discovery, Nuffield
15 Department of Population Health, University of Oxford, Oxford, UK

16 ⁶ KG Jebsen Centre for neurodevelopmental disorders, University of Oslo, Oslo, Norway

17 ⁷ Department of Psychiatry and Psychotherapy, University of Tübingen, Tübingen, Germany

18
19 * Corresponding authors:

20 Martina J. Lund and Tobias Kaufmann, PhD

21 Email: m.j.lund@medisin.uio.no, tobias.kaufmann@medisin.uio.no

22 Postal address: OUS, PoBox 4956 Nydalen, 0424 Oslo, Norway

23 Telephone: +47 23 02 73 50, Fax: +47 23 02 73 33

24
25
26 Counts:

27 Abstract: 241 words

28 Main text body: 4926 words

29 Figures: 5

30
31 Keywords:

32 Directed functional connectivity

33 Brain Development

34 Dynamic graphical models

35 Resting-state fMRI

36 The Healthy Brain Network

45 **Abstract**

46 Mental disorders often emerge during adolescence and have been associated with age-related
47 differences in connection strengths of brain networks (static functional connectivity),
48 manifesting in non-typical trajectories of brain development. However, little is known about
49 the direction of information flow (directed functional connectivity) in this period of functional
50 brain progression. We employed dynamic graphical models (DGM) to estimate directed
51 functional connectivity from resting state functional magnetic resonance imaging data on
52 1143 participants, aged 6 to 17 years from the healthy brain network (HBN) sample. We
53 tested for effects of age, sex, cognitive abilities and psychopathology on estimates of direction
54 flow. Across participants, we show a pattern of reciprocal information flow between visual-
55 medial and visual-lateral connections, in line with findings in adults. Investigating directed
56 connectivity patterns between networks, we observed a positive association for age and
57 direction flow from the cerebellar to the auditory network, and for the auditory to the
58 sensorimotor network. Further, higher cognitive abilities were linked to lower information
59 flow from the visual occipital to the default mode network. Additionally, examining the
60 degree networks overall send and receive information to each other, we identified age-related
61 effects implicating the right frontoparietal and sensorimotor network. However, we did not
62 find any associations with psychopathology. Our results revealed that the directed functional
63 connectivity of large-scale brain networks is sensitive to age and cognition during
64 adolescence, warranting further studies that may explore trajectories of development in more
65 fine-grained network parcellations and in different populations.

66 **Introduction**

67 The brain undergoes tremendous changes throughout life, where childhood and adolescence is
68 a particularly sensitive developmental period for brain maturation processes (Blakemore,
69 2012). A vital part of the brain's maturation happens in the functional networks that show
70 pronounced reorganization in order to facilitate neural efficiency and integration of
71 information, as indicated by functional magnetic resonance imaging (fMRI) studies in healthy
72 children and young individuals as well as in clinical populations in the same age range (Insel,
73 2010; Keshavan, Giedd, Lau, Lewis, & Paus, 2014; Kolskar et al., 2018; Rausch et al., 2016;
74 Schweinsburg, Nagel, & Tapert, 2005). This supports that this time period is a sensitive
75 phase, where there is large alterations in the functional interconnections between brain
76 regions, denoting the functional connectome, that link to when different mental disorders
77 emerge (Insel, 2010).

78 The primary method to study the functional connectome so far has been to estimate
79 static functional connectivity between brain regions, where research has shown that the
80 functional interconnections in healthy children and adolescents become more specialized (Li,
81 Deng, He, Zhai, & Jia, 2019). Resting-state networks (RSNs) also become more coherent and
82 stable during this time-period (Hoff, Van den Heuvel, Benders, Kersbergen, & De Vries,
83 2013), and evidence has indicated aberrant connectivity in individuals with pre-clinical
84 psychiatric symptoms (Kaufmann et al., 2017), which is in line with the brain dysconnectivity
85 hypothesis in mental disorders (Connolly et al., 2013; Di Martino et al., 2011; Friston & Frith,
86 1995; Hamm et al., 2014). Recently, estimating connectivity direction (Friston, Moran, &
87 Seth, 2013) has received interest as a field, as it could give new knowledge about the
88 connections between brain regions by yielding insight into the directionality in neural
89 information flow. For instance, Riley et al. (2018) examined connectivity direction with the
90 use of task- fMRI in a neurodevelopmental sample, where they observed differences between

91 sexes in relation to how memories are encoded in the hippocampus. In another
92 neurodevelopmental study by Hwang, Velanova, and Luna (2010), the authors observed that
93 improvements in inhibitory control were linked to strengthening of top-down connectivity for
94 regions implicated in cognitive control networks, while similar findings were found in
95 relation to top-down processing for a language network (Bitan et al., 2006). Further, it has
96 been shown that there are differences in directionality in adolescent boys with externalizing
97 behavior disorders in comparison with controls (Shannon, Sauder, Beauchaine, & Gatzke-
98 Kopp, 2009). Likewise, alterations in connectivity direction in resting-state fMRI (rsfMRI)
99 data have been observed for clinical samples, where children with autism and Attention
100 Deficit Hyperactivity Disorder (ADHD) show a common pattern implicating Broca's area
101 across clinical groups, along with distinctive patterns of functional connectivity specific for
102 given disorders (Henry et al., 2019). In addition, others have found higher directed
103 connectivity from left to right superior parietal lobule to be associated with an improved shift
104 and emotional control across healthy children and clinical participants (Dajani et al., 2019).

105 However, the literature on connection directionality is scarce, calling for validation of
106 earlier findings and for new insights using novel approaches. In particular, we do not
107 currently know how and to what extent the direction flow in the communication between
108 brain networks is implicated in mental traits and disorders, including cognitive abilities.
109 Given that cognitive deficits are seen across mental disorders, connecting these behavioral
110 and clinical characteristics is crucial for gaining a better understanding of how higher-order
111 processing is characterized in children and adolescence. Such integrative understanding is
112 also important given that no consensus has been reached when it comes to the disorder-
113 specific connectivity alterations that characterize particular mental disorders and the known
114 overlap of symptoms (Craddock & Owen, 2010; Jollans & Whelan, 2018) and genetic
115 pleiotropy between disorders (Lee et al., 2019; Smeland et al., 2019).

116 Dynamic graphical models (DGM) is a Bayesian approach for examining directed
117 functional connectivity using dynamic linear models (DLM) (Schwab et al., 2018). As such, it
118 implements a state space model that is linear and Gaussian in form. This includes statistically
119 stationary properties as it uses a hidden Markov modelling approach, although it incorporates
120 time varying coefficients and as a result can provide information about directionality in the
121 form of a binary view of coupling between two brain regions for each connectivity direction.

122 Here, we used DGM and publicly available rsfMRI data from the Healthy Brain
123 Network (HBN) project (Alexander et al., 2017) to study brain network information flow in
124 children and adolescents and its associations with age, sex, cognitive abilities and
125 psychopathology. We hypothesized that information flow would have a positive association,
126 and be strengthened with increasing age (Bitan et al., 2006; Hwang et al., 2010), that there
127 would be differences between females and males in the maturation of brain networks and its
128 information flow (Riley et al., 2018), as well as alterations associated with information flow
129 for control networks as these nodes are central to a range of disorders (Cortese, Kelly, & Di
130 Martino, 2012; Eisenberg & Berman, 2010; Francx et al., 2015; Geiger et al., 2016; Li et al.,
131 2017; Zhao, Swati, Metmer, Sang, & Lu, 2019).

132 **Methods**

133 **Study samples**

134 The HBN is a project organized by the Child Mind Institute (Alexander et al., 2017) and is a
135 resource targeting novel insight into the critical time period when psychiatric and mental
136 disorders emerge. The HBN consortium aims to include 10,000 individuals in the age range
137 of 5-21 years from the New York area, where participants are included by use of
138 announcements that are distributed to community members, educators, local care providers
139 with the addition of sending information via email lists and events to parents, encouraging

140 participation of children with clinical concerns to this study (Alexander et al., 2017). Data on
141 these individuals include a package consisting of MRI scanning, genetics,
142 electroencephalography (EEG), eye-tracking, as well as biological testing and a
143 neuropsychological battery consisting of cognitive, lifestyle indices, behavioral and
144 psychiatric domains in addition to actigraphy and voice and video interviews (Alexander et
145 al., 2017). Exclusion criteria include serious neurological disorders, neurodegenerative
146 disorders, acute encephalopathy, hearing or visual impairment, lifetime substance abuse that
147 necessitated chemical replacement therapy/acute intoxication at time of study, recent
148 diagnosis of a severe mental disorder or manic/psychotic episode within the last 6 months
149 without ongoing treatment, in addition to the onset of suicidality/homicidality where there is
150 no current, ongoing treatment (Alexander et al., 2017). All participants over the age of 18
151 years provided signed informed consent, while legal guardians signed informed consent for
152 participants under the age of 18, in addition to participants giving a written assent (Alexander
153 et al., 2017). The Chesapeake Institutional Review Board approved the study ([https://www.
154 chesapeakeirb.com/](https://www.chesapeakeirb.com/)).

155

156 MRI acquisition and preprocessing

157 MR data was collected by the study team of HBN, where we included MRI data from the
158 following sites; Rutgers University Brain Imaging Center (RUBIC), Citigroup Biomedical
159 Imaging Center (CBIC) and a mobile scanner located in Staten Island. MRI data was
160 collected using one scanner at each site, giving a total of 3 scanners comprising our sample.
161 Rutgers applied a Siemens 3T Tim Trio scanner, while CBIC utilized a Siemens 3T Prisma,
162 and both sites applied the same MRI parameters, where resting- state blood-oxygen-level-
163 dependent (BOLD) fMRI data was collected for each subject using a T2*-weighted BOLD
164 echo-planar imaging (EPI) sequence with a repetition time (TR) of 800ms, echo time (TE) of

165 30ms, multiband acceleration factor = 6, 60 number of slices with the rsfMRI session
166 consisting of 375 volumes and with voxel size= 2.4×2.4×2.4 mm. The third mobile scanner
167 located in Staten Island used a 1.5T Siemens Avanto system equipped with 45 mT/m
168 gradients (Alexander et al., 2017), where the following parameters were implemented; TR=
169 1.45s, TE=40ms, multiband acceleration factor = 3, number of volumes=420, slices= 54,
170 resolution in mm= 2.5×2.5×2.5 mm (for more information about the MRI parameters, see
171 http://fcon_1000.projects.nitrc.org/indi/cmi_healthy_brain_network/MRI%20Protocol.html).
172 Raw imaging data was downloaded from the HBN database
173 ([http://fcon_1000.projects.nitrc.org/indi/cmi_healthy_brain_network/sharing_neuro.html#Dir](http://fcon_1000.projects.nitrc.org/indi/cmi_healthy_brain_network/sharing_neuro.html#Directory%20Down)
174 [ect%20Down](http://fcon_1000.projects.nitrc.org/indi/cmi_healthy_brain_network/sharing_neuro.html#Directory%20Down)), and analyzed on the secure data storage and computing facilities (TSD,
175 <https://www.uio.no/tjenester/it/forskning/sensitiv>) at University of Oslo. Image processing
176 tools, based largely on Smith et al. (2013), were used for the functional data while T1-
177 weighted data, which was applied as an intermediate in the registration, was processed using
178 FreeSurfer 5.3 (<http://freesurfer.net>), including removal of non-brain tissue.

179 As part of the HBN MRI protocol, multiple T1 weighted sequences were acquired for
180 each subject, and we used MRIQC version 0.14.2 (Esteban et al., 2017) for automated quality
181 assessment (N=2427, CUNY scanning site was included for the MRIQC stage, yet this site
182 was dropped at a later stage due the low sample size, N=22). From this, T1 weighted images
183 with the best image quality metrics, based on the classifier ratings, were used as input for
184 registration, while structural scans that were flagged as low quality (classifier rating score
185 >0.5, N=160) were manually checked and excluded (N=117). In addition, 22 subjects had
186 errors when they were run through FreeSurfer and after manually inspecting these datasets,
187 these were also omitted due to motion artefacts and/or having MRI findings disrupting the
188 segmentation pipeline in FreeSurfer. We also made a global mask of the T1 data where we

189 manually checked subjects that had low coverage, excluding another 95 subjects leaving a
190 total of 2171 datasets that had a usable T1w sequence for registration.

191 Two of the MRI sites, RUBIC and CBIC, had two resting-state scans acquired as part
192 of the same MRI session. As the DGM method benefits from more time points, we merged
193 the time series for subjects with two resting state scans together to leverage all available
194 resting-state data. This was done prior to implementing feat as a means of optimizing the data
195 by improving the spatial alignment between the sessions, and to have the full set of volumes
196 to inform FIX.

197 Furthermore, the first five volumes for the fMRI dataset were discarded. We
198 preprocessed fMRI data using FSL 6.0.3 (<http://fsl.fmrib.ox.ac.uk>), including motion
199 correction and brain extraction. FSL's FEAT (Woolrich, Ripley, Brady, & Smith, 2001)
200 included spatial smoothing with a Gaussian kernel FWHM of 6 mm and a high-pass filter
201 cutoff of 100. FMRIB's Nonlinear Image Registration tool (FNIRT) was used to register
202 fMRI volumes to standard space (MNI-152) with the T1w volumes as intermediates.

203 We also implemented a cleaning step for fMRI data, where we made a global mask for
204 the fMRI datasets (which indicated data coverage across participants), and from this we
205 excluded 128 of 1813 datasets with poor coverage. To reduce the influence of noise in the
206 data and increase the tSNR (Kaufmann et al., 2017), we removed artefacts by use of ICA-
207 AROMA, a classifier that identifies and removes motion specific noise in fMRI data (Pruim,
208 Mennes, Buitelaar, & Beckmann, 2015; Pruum, Mennes, van Rooij, et al., 2015). Afterwards,
209 ICA was rerun and FSL's FIX (FMRIB's ICA-based X-noisiefier (Griffanti et al., 2014;
210 Salimi-Khorshidi et al., 2014)), was used with the recommended threshold of 20 to remove
211 remaining motion confounds and other artefacts in the data. Further, data was temporally
212 demeaned and variance normalized (Beckmann & Smith, 2004), and the quality controlled
213 fMRI dataset (N=1685) was submitted to a group ICA, utilizing FSL's Multivariate

214 Exploratory Linear Optimized Decomposition into Independent Components (MELODIC)
215 tool (Beckmann & Smith, 2004; Hyvärinen, 1999), where 25 components were extracted from
216 the ICA and used for further analysis. Dual regression was applied to estimate individual
217 spatial maps and corresponding time series from the group ICA (Beckmann & Smith, 2004;
218 Filippini et al., 2009), which were used as input for the DGM analysis.

219

220 Mental and cognitive measures

221 From the HBN data release, N=1685 participants were included after quality assessment. Out
222 of these, information on age at MR was missing for N=45, sex for N=9, and cognitive/clinical
223 information for 496 individuals. The participants were 5-22 years (mean: 11.5, years, sd: 3.51
224 years) and 37.9% were females. This data was used to study group-level patterns of dFC
225 (average connectivity matrix). For the subsequent associations with age, sex, cognition and
226 mental health, we restricted the analysis to a subset based on data availability. Thus, the final
227 sample for the association analyses comprised N=1143, individuals aged 6-17 years (mean:
228 10.7 years, sd: 2.62 years, 37.4% females, where N=83 were from the Staten Island site,
229 N=503 from CBIC and N=557 from RUBIC scanning site (see SI SFig.2 for age distributions
230 within scanner sites). A large proportion of the sample had a diagnosis (N=1012), while
231 N=105 did not have a diagnosis, N=23 dropped out before a diagnosis could be determined,
232 and N=3 was missing information for clinical consensus diagnosis data and had as such not
233 received a diagnosis. Broadly, the majority of patients included in our analysis had disorders
234 in the following categories where comorbidities are included. Accordingly, there is a higher N
235 than the total number of subjects for each diagnosis category given here: Neurodevelopmental
236 disorders (N=1526), anxiety disorders (N=557), disruptive, impulsive control and conduct
237 disorders (N=171), elimination disorders (N=111), and depressive disorders (N=115), see SI;
238 SFig. 1 for further details.

239 We used the full-scale intelligence quotient (FSIQ) from the Wechsler Intelligence
240 Scale for Children (WISC-V) taken for participants aged 6-17 years as a proxy for cognitive
241 ability. This composite score includes the following domains; visual spatial, verbal
242 comprehension, fluid reasoning, working memory, and processing speed (Wechsler, 2003).
243 Mental health was measured on a continuum including both healthy subjects and patients as it
244 is difficult to uncover robust findings for psychiatric diagnosis that constitutes heterogeneous
245 disorders, showing a wide range in symptoms, severity, duration and prognosis, and as
246 patients often have more than one diagnosis. Such heterogeneity is also reflected in the brain,
247 making the search for biological markers a complex task. As such, for mental health, we
248 performed a principal component analysis (PCA) on The Extended Strengths and Weaknesses
249 Assessment of Normal Behavior (E-SWAN), which has been shown to be a valid
250 psychometric assessment tool for investigating behavior underlying DSM disorders
251 (Alexander, Salum, Swanson, & Milham, 2020). E-SWAN domains include depression,
252 social anxiety, disruptive mood dysregulation disorder (DMDD), and panic disorder. We
253 excluded 3 of the items relating to panic disorder from the questionnaire that had a high
254 degree (90%) of missing values, giving a total of 62 items for the PCA analysis. The
255 remaining items had available data for 2626 participants with no missing values. We
256 performed PCA using the “prcomp” function in R, where the first PC, often denoted as the p-
257 factor or pF (Caspi et al., 2013), explained 43.6% of the variance (Figure 1). From the
258 loadings from the PCA, this component was associated with items related to self-control and
259 depression/anxiety (Figure 1). In accordance with other studies showing more than one factor
260 being of importance (Alnaes et al., 2018; Mallard et al., 2019), we also included the second
261 principal component referred to as pF₂, which was associated with items relating to mood
262 dysregulation. This component explained 11.3% of the variance.

263



264

265 *Figure 1: Principal component analysis performed on the ESWAN questionnaire taken as*
 266 *part of the HBN protocol. For visualization purposes, only the components included in our*
 267 *analysis are shown. We used the first two principal components as proxies of*
 268 *psychopathology, referred to as “pF” and “pF₂”.*

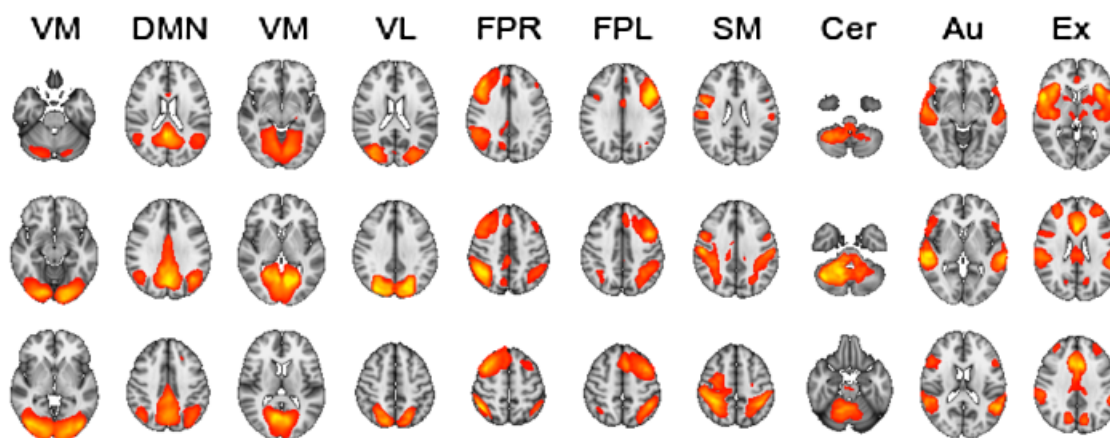
269

270 Network analysis

271 We chose ten resting-state networks from the model order of 25 for inclusion in the dFC
 272 analysis. These networks were chosen based on spatial correlation and manually ensuring

273 overlapping ICs with the ten RSNs reported by Smith et al. (2009). The ten networks
274 comprised the default mode (DMN), cerebellar (Cer), visual occipital (VO), visual medial
275 (VM), visual lateral (VL), right frontoparietal (FPR), left frontoparietal (FPL), sensorimotor
276 (SM), auditory (Au), and the executive control (Ex) network (Figure 2). These networks were
277 also used in previous DGM studies (Lund et al., 2020; Schwab et al., 2018). Including the
278 same nodes allowed us to compare results with prior findings and to integrate the current
279 results obtained from a childhood and adolescent sample with previous adult studies. The
280 included timeseries for each node were mean centered before estimating dFC from individual
281 level RSN time series using the DGM package v1.7.2 in R. DGM is a set of regressions with
282 time-varying coefficients (DLMs) for every receiving node. The receiver node refers to the
283 network that receives information from a sending node that transmits information between a
284 node pair. For each DLM, all possible models for the sender nodes are tested and the model
285 with the highest model evidence is selected. Consequently, a model is stated by the sending
286 networks of a node, giving a binary outcome. The outcome indicates if there is an influence or
287 not between two networks. DGM has uncovered meaningful trajectories in rsfMRI mice data
288 where DGM revealed a link between areas in the hippocampus that fed information to the
289 cingulate cortex, in line with previous studies using viral tracers to delineate directed
290 anatomical connectivity in mice (Schwab et al., 2018). Additionally, even with systemic
291 hemodynamic lag confounds being introduced in the data, network simulations demonstrated
292 a sensitivity of 72%–77% for the DGM approach (Schwab et al., 2018).

293



294

295 *Figure 2: group-level maps for the 10 selected independent components included in the*
296 *analysis (where the z-score maps threshold is set at 4).*

297

298 Statistical analysis

299 We included all available rsfMRI scans for the group ICA, as a higher number of subjects is
300 beneficial for yielding more robust ICs, while restricting the association analyses to the subset
301 that had all covariates available. We performed the same analysis as previously reported in an
302 adult sample (Lund et al., 2020), examining dFC on the edge- and node-level. Edge-level
303 analysis deployed logistic regression for every connection of the directed network using
304 directed connectivity as the response variable and testing for associations with age, age-
305 orthogonalized age squared (age^2 , using the poly function in R), sex, cognitive abilities,
306 mental health, tSNR, motion and scanning site (as data was acquired at multiple scanners).
307 These covariates were included into one model (see SI; SFig.5, for additional analyses
308 examining potential multicollinearity for covariates included in the model). P-values were
309 Bonferroni corrected for a number of 90 analyses on the edge-level (alpha level of 0.05). In
310 addition, we performed node-level analysis to examine which networks overall send and
311 receive information to each other (Lund et al., 2020). We calculated the number of output
312 connections or outgoing edges (referred to as out-degree) and the number of input

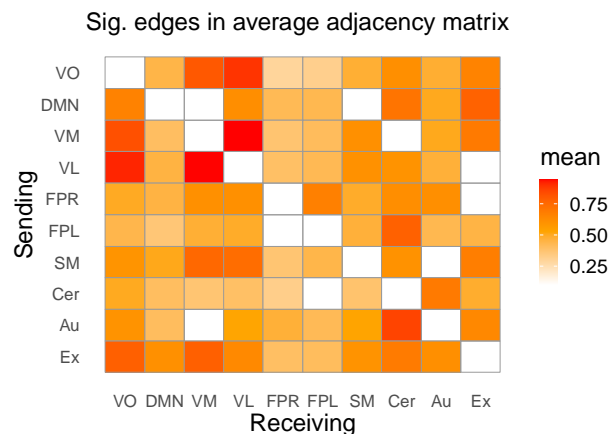
313 connections or incoming edges (referred to as in-degree) for a given node. We performed
314 linear regression using in-degree and out-degree as dependent variables and the same
315 independent variables as used in the logistic regression on edge-level. P-values were
316 Bonferroni corrected for a number of 10 analysis on the node-level (alpha level of 0.05).

317

318 Results

319 Figure 3 depicts the average directed functional connectivity matrix across all individuals.
320 Several connections indicated bi-directionality in information flow, especially directionality
321 estimates for the visual lateral and visual medial networks where information flow from VM
322 to VL was present in 94.4% of individuals, while connection from VL to VM was present in
323 94.2%. In addition, there was overall a high number of participants that showed a reciprocal
324 relationship between the VO to VM and VL (VO to VL: 89.1%, VO to VM: 80.2%) and
325 opposite (VL to VO: 91.5%, VM to VO: 82.7%). These bi-directional relationships are in
326 alignment with patterns of information flow found in adults from the UK Biobank sample
327 (Lund et al., 2020). However, we did not observe the bi-directional information flow found
328 previously for adults between the DMN and FPR network. Further, when observing receiver
329 networks, the FPL showed the same as found for adults, that it did not receive information to
330 a large extent (Lund et al., 2020), coherent with our findings in youths. Additionally, the edge
331 most present across all individuals, aside from the visual networks, was Cer which receives
332 input from the Au (85.6%). This connection was also relatively strongly expressed in the
333 other direction (68.6%). Moreover, the FPL sent information to Cer, and this edge was
334 present in 77.7% of individuals. Yet, in this neurodevelopmental sample we did not observe
335 that Cer and Au overall were mostly receivers, as found for adults (Lund et al., 2020).

336



337

338 *Figure 3: Average directed connectivity matrix across HBN subjects showing the significant*
339 *proportions of edges between the 10 RSNs included in the analysis; VO, visual occipital;*
340 *DMN, default mode; VM, visual medial; VL, visual lateral; FPR, frontoparietal right; FPL,*
341 *frontoparietal left; SM, sensorimotor; Cer, cerebellum; Au, auditory; Ex, executive control*
342 *network. The y-axis indicates the sender node, and the x-axis indicates the receiver nodes.*
343 *Significance was assessed using a binomial test as implemented in the binom.nettest function*
344 *in R, with a predefined FDR threshold of 5% and the hypothesized probability $p_0 = .56$.*

345

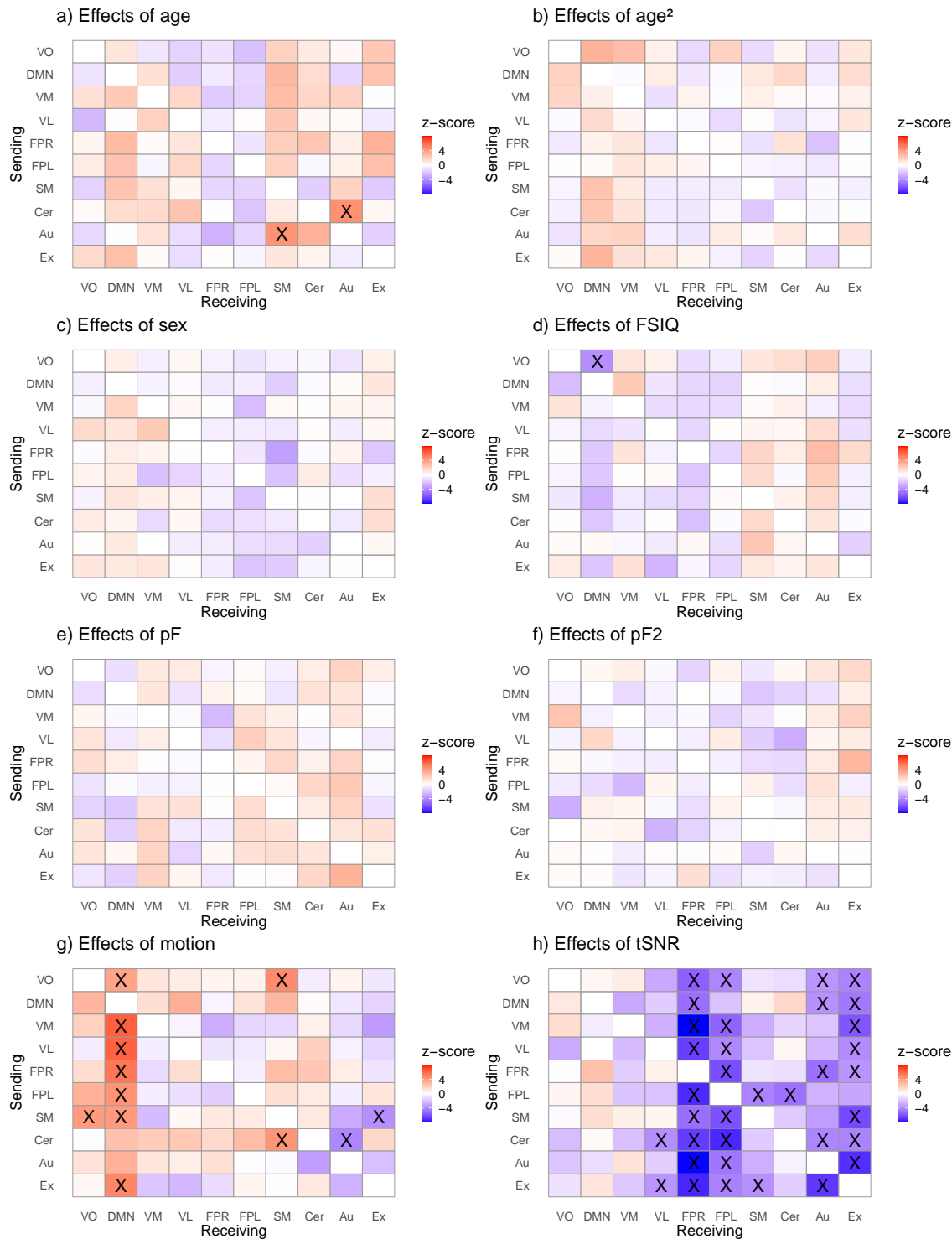
346 Effects of age and cognition on dFC measures

347 Edge-level analysis of dFC showed significant effects of age, in line with our hypothesis of
348 age being associated with the functional networks' maturation processes occurring in
349 childhood and adolescence (Figure 4; SI Tables 1-6 show z-scores and p-values and SFig.3-4
350 show effects of scanner). Specifically, we observed a positive association with age and dFC
351 from the Cer to the Au network. Correspondingly, the Au sends more information with higher
352 age to the SM node. For cognitive test performance and dFC, we observed a significant
353 negative association between VO and DMN, with the DMN receiving less information from
354 the VO network with higher cognitive test performance.

355 On the node-level, we assessed similar phenotypic associations for the out-degree and
356 in-degree of the networks. Confirming edge-level results, age was significantly associated
357 with the in-degree (number of input connections) of SM (fig.4b), indicating that the SM
358 network overall receive more information with increasing age. Additionally, for out-degree
359 (number of output connections), there was a significant positive association for age and FPR,
360 signifying that the FPR network overall sends more information with increasing age. As
361 expected, there was significant effects for the control variables scanning site (SFig.3-4), tSNR
362 and motion on edge and node-level.

363 Based on prior studies, we expected that mental health would be associated with
364 information flow for control networks, however, this was not observed. We also expected
365 sex-related differences in the maturation of brain networks, but this was not found.

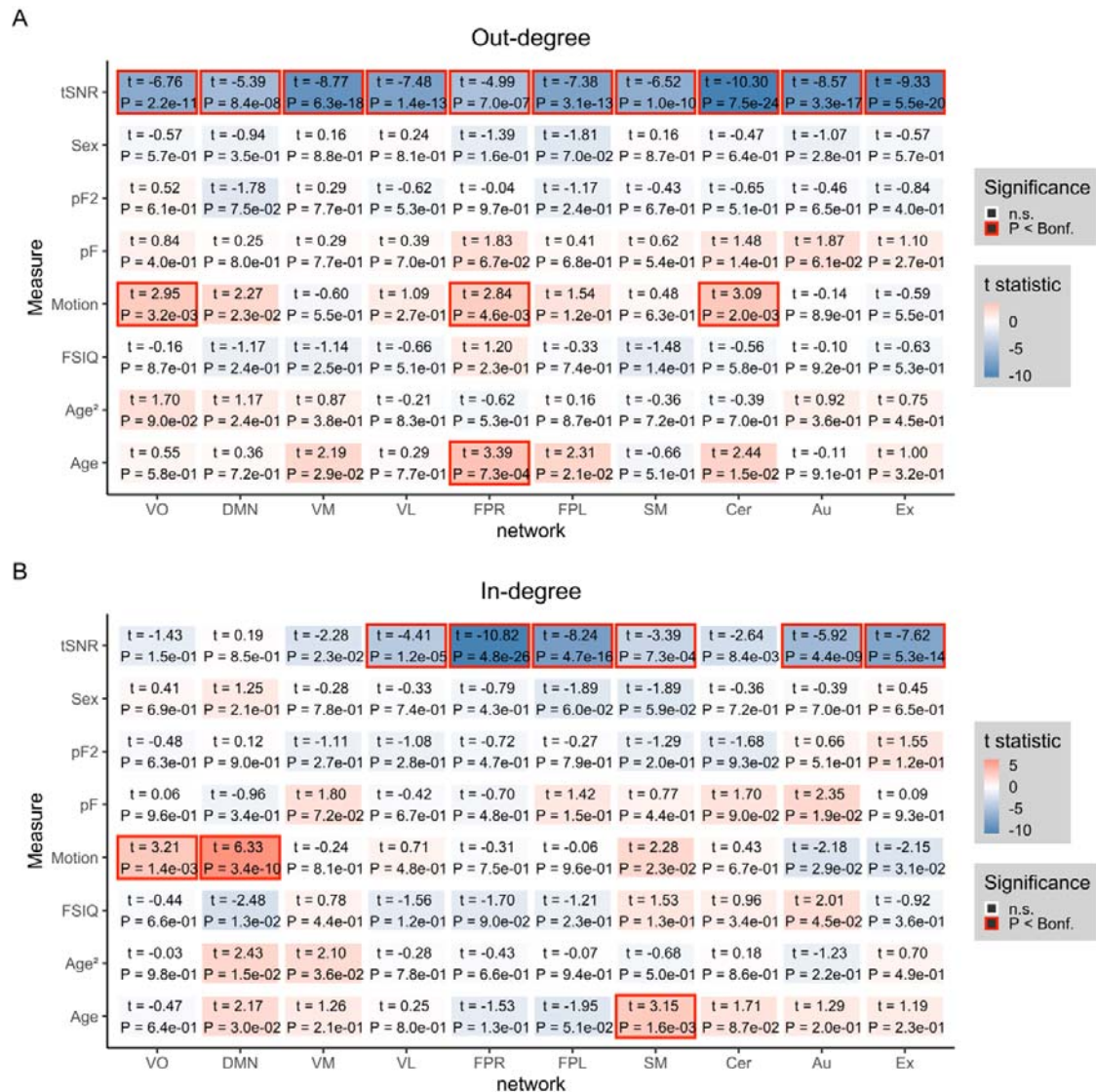
366



367

368 *Figure 4: Matrices showing the effects of age (a), age² (b), sex (c), intellectual abilities*
 369 *(FSIQ) (d), mental health (pF and pF₂) (e,f), motion (g), and tSNR (h) on directed*
 370 *connectivity. The analysis was performed in HBN data that had no missing values (N = 1143,*

371 6–17 years, $df = 1132$). Significant edges following Bonferroni correction are marked as X.
 372 The legend shows the 10 RSNs included in the analysis; VO, visual occipital; DMN, default
 373 mode; VM, visual medial; VL, visual lateral; FPR, frontoparietal right; FPL, frontoparietal
 374 left; SM, sensorimotor; Cer, cerebellum; Au, auditory; Ex, executive control network. The y-
 375 axis indicates the sender node, while the x-axis refers to the receiving node. The colors reflect
 376 the z-value for the corresponding effects where red indicates a positive association and blue a
 377 negative association.



379

380 *Figure 5: Associations on the node level (N=1143, 6-17 years, df= 1132). a) Out-degree*
381 *matrix with corresponding effects of covariates age, age², sex, cognition (FSIQ), mental*
382 *health (pF and pF₂), tSNR, and motion in HBN data. B) In-degree matrix with corresponding*
383 *effects for the same covariates as in panel a). The colors reflect the t-value for the*
384 *corresponding effect where numbers inside the boxes indicate t-statistic and p-value, and*
385 *significant effects are marked with a red border following Bonferroni correction (p < .05).*

386

387 Discussion

388 Our analysis revealed marked dFC patterns for the visual networks. Specifically, we observed
389 a reciprocal information flow between the VM and VL in the investigated sample of children
390 and adolescence. This is in alignment with previous findings in adults (Lund et al., 2020;
391 Schwab et al., 2018), and coherent with primary sensory and motor cortical regions maturing
392 first, and being present early on in children (Casey, Tottenham, Liston, & Durston, 2005). In
393 contrast, we did not find that the cerebellum or auditory networks are mostly receivers of
394 information as observed in adults (Lund et al., 2020; Schwab et al., 2018). However, apart
395 from the visual circuits, the Cer received most information overall from the other transmitter
396 networks, potentially indicating its role as a receiver, as found for adults.

397 We observed significant associations between age and directed connectivity both at
398 edge and node-level. At the edge-level and with increasing age, the Cer had higher
399 information flow to the Au network, while the Au sent more information to the SM network.
400 Of note, these connections demonstrating age-dependent dFC have been implicated in
401 neurodevelopmental disorders such as autism, which is characterized by symptoms related to
402 hyper- and hypo sensitivity in relation to sensory modalities (Marco, Hinkley, Hill, &
403 Nagarajan, 2011). Moreover, it has been reported that the cerebellar network is mostly a
404 receiver of information from other attention and memory related regions in children with

405 ADHD when estimating directed connectivity in rsfMRI using a seed-based approach (Zhao,
406 Zheng, Yang, & Tian, 2017). The average connectivity across participants indicated that the
407 FPL sent information to Cer in 77.7% of the participants, which is in line with the
408 aforementioned findings. Hence, this could be an interesting avenue to investigate in relation
409 to potential biomarkers in future studies.

410 Likewise, on the node-level, the SM received more information with increasing age,
411 while the FPR sent more information with higher age to the other networks overall. These
412 results indicate that directionality estimates in both bottom-up and top-down processing are
413 involved in the transitional phase from child to adulthood across patients and healthy
414 individuals. This is in line with prior findings implicating these networks in normal functional
415 development (Muetzel et al., 2016). Similarly, alterations in the right frontoparietal network
416 has been associated with ADHD, where children and adolescent ADHD combined type
417 patients show a reduction in FPR regions, when probing spatial working memory by use of
418 task-fMRI (Silk et al., 2005; Vance et al., 2007).

419 For cognitive abilities and dFC, we observed a significant negative association
420 between VO and DMN, with the DMN receiving less information from the VO network with
421 higher cognitive test performance. This could indicate that individuals that were more focused
422 on the task at hand benefited from less information flowing from VO to DMN, potentially
423 facilitating effective whole-brain connectivity which has been linked to cognitive efficiency
424 (van den Heuvel, Stam, Kahn, & Hulshoff Pol, 2009). However, it is challenging to delineate
425 information flow as this could be disrupted for many connections and give rise to different
426 alterations in connectivity. Nonetheless we did expect to observe associations for control
427 networks in relation to cognitive abilities as this has been reported by others (Cole, Yarkoni,
428 Repovs, Anticevic, & Braver, 2012; Li & Tian, 2014; R. Li, Zhang, Wu, Wen, & Han, 2020).
429 Interestingly, the core executive function cognitive flexibility, has in healthy adults been

430 associated with strong within-system connectivity in higher order systems and from these
431 networks to primary-sensory motor systems when estimating dFC (Chen et al., 2019). Altered
432 within network connectivity in relation to cognitive flexibility and in general has also been
433 reported for neurodevelopmental disorders (Dajani et al., 2019; Henry et al., 2019). Here we
434 estimated information flow between networks with different functions rather than within-
435 system connectivity (with the exception of the visual networks). In addition, we used a
436 normed cognitive composite test score as a proxy for cognition. However, this may not be an
437 optimal approach as test norms could have limitations when it comes to representativeness
438 and number of subjects included in the normative sample, making it less sensitive for clinical
439 populations and for the lowest scoring percentile.

440 We utilized two general p factors for measuring symptoms in this sample. These
441 psychopathology loadings, were related to self-control and depression/anxiety (pF) and items
442 pertaining to mood dysregulation (pF₂). Top-down control functions for cortico-limbic
443 regions have been linked to modifications for symptoms relating to mood dysregulation in
444 development. For instance, it has been shown that increased centromedial amygdala-rostral
445 anterior cingulate cortex functional connectivity is related to a higher level of anxiety and
446 depression symptoms during early adulthood, while increased structural connectivity in
447 centromedial amygdala-anterior ventromedial prefrontal cortex white matter was linked to
448 augmented symptoms of anxiety and depression during late childhood (Jalbrzikowski et al.,
449 2017). We did not observe significant associations between dFC and symptom burden for any
450 of the networks. Our dimensional approach of estimating PCA on symptom data represents
451 both healthy subjects and individuals with a psychiatric disorder on a symptom continuum
452 rather than as cases and control. Such a dimensional approach may better capture intermediate
453 phenotypes which map to brain biology and the neuronal mechanisms underlying the
454 symptoms, compared to diagnostic categories (Hengartner & Lehmann, 2017; Krueger &

455 Bezdjian, 2009). While the lack of significant associations in our study indicates that
456 between-network dFC in large-scale brain networks is not sensitive to mental health in this
457 sample, future research will need to investigate dFC in distinct subnetworks and by different
458 symptom measures, and also consider structural connectivity.

459 We expected to find differences between sexes in relation to directed connectivity as
460 this has been found previously in adolescence (Riley et al., 2018) using task-fMRI, and when
461 examining dFC in adults (Lund et al., 2020). However, we did not find any significant sex
462 differences in dFC on edge- or node-level in rsfMRI. This may partly relate to sample
463 characteristics such as the uneven sex distribution and the inclusion of patients in our sample.

464

465 Limitations

466 As with any MRI study, participant motion during scanning may confound the results,
467 especially as it is known that both young individuals and those with a psychiatric diagnosis on
468 average move more (Satterthwaite et al., 2012). We therefore implemented a stringent
469 correction pipeline, where we implemented several steps of ICA and machine learning based
470 cleaning (FIX and AROMA). We also included the mean relative motion measure from FSL
471 as a covariate in our analysis step. Another relevant confound effect that could potentially
472 bias our results and the comparison to previous work is variability in the ICA decompositions.
473 We performed ICA in the study sample and selected components based on similarity to
474 components reported by Smith et al. (2009). While this approach yielded overall good
475 comparison to previous work, subtle differences between decompositions may retain and
476 might impact the derived dFC patterns. For instance, sensorimotor nodes were divided into
477 three independent components where the node with the best spatial overlap with the SM
478 component in Smith et al. (2009) was chosen. Most likely including another sensorimotor
479 related node would change the results of our analysis. Hence, our results call for follow-up

480 analysis in more fine-grained networks. In this framework, different ways to parcellate the
481 brain could be tested.

482 The majority of the individuals in the sample were diagnosed with a child and
483 adolescence mental disorder. This was beneficial when examining associations of
484 psychopathology on directionality estimates as it yielded a high number of patients in each
485 group, but makes it difficult to delineate if average patterns of information flow are for typical
486 or non-typical functional development. In addition, medication may have had an effect on our
487 results, as participants were asked to discontinue stimulant medication but were still enrolled
488 if they chose not to discontinue due to personal reasons or if recommended by their physician.

489 On a methodological note, DGM reflects instantaneous relationships and does not only
490 look at lagged relationships, however sensitivity of DGM drops depending on the total offset
491 between a node pair and can as such influence the estimation of these interactions. Further,
492 DGM estimates binary connections, which may have reduced the sensitivity of the association
493 analyses.

494 Lastly, whether differences in findings compared to previous studies in adults are of
495 methodological origin, such as differences in preprocessing pipelines or network definitions,
496 or can be explained by differences in dynamic connectivity between children and adults
497 remains to be further investigated.

498

499 Conclusions

500 To conclude, using a sample of children and adolescents, we showed that the direction of the
501 information flow was age dependent for auditory, sensorimotor and cerebellar connections. In
502 addition, the FPR had a higher degree of input connections with higher age. These findings
503 contribute to the existing knowledge in the brain development field, and warrant further
504 studies for replication in healthy samples as well as other clinical populations.

505

506 Funding

507 The authors were funded by the Research Council of Norway #276082 (LifespanHealth),
508 #223273 (NORMENT), #249795, #298646, #300767, #283798; H2020 European Research
509 Council #802998 (BRAINMINT); The South-East Norway Regional Health Authority
510 #2019101, #2019107, #2020086; Swiss National Science Foundation #171598

511

512 Financial disclosures

513 OAA is a consultant for HealthLytix.

514

515 Data and code availability

516 The data incorporated in this work were gathered from the open access Healthy Brain
517 Network resource. Software needed to estimate directed connectivity is available at
518 <https://github.com/schw4b/DGM>.

519

520 Acknowledgements

521 This manuscript was prepared using a limited access dataset obtained from the Child Mind
522 Institute Biobank, the HBN resource (<http://www.healthybrainnetwork.org>). Its initiatives are
523 supported by philanthropic contributions from the following individuals, foundations and
524 organizations: Margaret Bilotti; Brooklyn Nets; Agapi and Bruce Burkard; James Chang;
525 Phyllis Green and Randolph Cōwen; Grieve Family Fund; Susan Miller and Byron Grote;
526 Sarah and Geoff Gund; George Hall; Jonathan M. Harris Family Foundation; Joseph P.
527 Healey; The Hearst Foundations; Eve and Ross Jaffe; Howard & Irene Levine Family
528 Foundation; Rachael and Marshall Levine; George and Nitzia Logothetis; Christine and
529 Richard Mack; Julie Minskoff; Valerie Mnuchin; Morgan Stanley Foundation; Amy and John

530 Phelan; Roberts Family Foundation; Jim and Linda Robinson Foundation, Inc.; The Schaps
531 Family; Zibby Schwarzman; Abigail Pogrebin and David Shapiro; Stavros Niarchos
532 Foundation; Preethi Krishna and Ram Sundaram; Amy and John Weinberg; Donors to the
533 2013 Child Advocacy Award Dinner Auction; Donors to the 2012 Brant Art Auction.

534 This manuscript reflects the views of the authors and does not necessarily reflect the
535 opinions or views of the Child Mind Institute.

536 This work was performed on the TSD (Tjeneste for Sensitive Data) facilities, owned
537 by the University of Oslo, operated and developed by the TSD service group at the University
538 of Oslo, IT-Department (USIT) (tsd-drift@usit.uio.no).

539

540

541 References

542

- 543 Alexander, L. M., Escalera, J., Ai, L., Andreotti, C., Febre, K., Mangone, A., . . . Milham, M.
544 P. (2017). An open resource for transdiagnostic research in pediatric mental health and
545 learning disorders. *Scientific Data*, 4(1). doi:10.1038/sdata.2017.181
- 546 Alexander, L. M., Salum, G. A., Swanson, J. M., & Milham, M. P. (2020). Measuring
547 strengths and weaknesses in dimensional psychiatry. *J Child Psychol Psychiatry*,
548 61(1), 40-50. doi:10.1111/jcpp.13104
- 549 Alnaes, D., Kaufmann, T., Doan, N. T., Cordova-Palomera, A., Wang, Y., Bettella, F., . . .
550 Westlye, L. T. (2018). Association of Heritable Cognitive Ability and
551 Psychopathology With White Matter Properties in Children and Adolescents. *JAMA*
552 *Psychiatry*, 75(3), 287-295. doi:10.1001/jamapsychiatry.2017.4277
- 553 Beckmann, C. F., & Smith, S. M. (2004). Probabilistic Independent Component Analysis for
554 Functional Magnetic Resonance Imaging. *IEEE Transactions on Medical Imaging*,
555 23(2), 137-152. doi:10.1109/tmi.2003.822821
- 556 Bitan, T., Burman, D. D., Lu, D., Cone, N. E., Gitelman, D. R., Mesulam, M. M., & Booth, J.
557 R. (2006). Weaker top-down modulation from the left inferior frontal gyrus in
558 children. *NeuroImage*, 33(3), 991-998. doi:10.1016/j.neuroimage.2006.07.007
- 559 Blakemore, S.-J. (2012). Imaging brain development: The adolescent brain. *NeuroImage*,
560 61(2), 397-406. doi:10.1016/j.neuroimage.2011.11.080
- 561 Casey, B. J., Tottenham, N., Liston, C., & Durston, S. (2005). Imaging the developing brain:
562 what have we learned about cognitive development? *Trends Cogn Sci*, 9(3), 104-110.
563 doi:10.1016/j.tics.2005.01.011
- 564 Caspi, A., Houts, R. M., Belsky, D. W., Goldman-Mellor, S. J., Harrington, H., Israel, S., . . .
565 Moffitt, T. E. (2013). The p Factor. *Clinical Psychological Science*, 2(2), 119-137.
566 doi:10.1177/2167702613497473

- 567 Chen, O. Y., Cao, H., Reinen, J. M., Qian, T., Gou, J., Phan, H., . . . Cannon, T. D. (2019).
568 Resting-state brain information flow predicts cognitive flexibility in humans. *Sci Rep*,
569 9(1), 3879. doi:10.1038/s41598-019-40345-8
- 570 Cole, M. W., Yarkoni, T., Repovs, G., Anticevic, A., & Braver, T. S. (2012). Global
571 connectivity of prefrontal cortex predicts cognitive control and intelligence. *J*
572 *Neurosci*, 32(26), 8988-8999. doi:10.1523/JNEUROSCI.0536-12.2012
- 573 Connolly, C. G., Wu, J., Ho, T. C., Hoeft, F., Wolkowitz, O., Eisendrath, S., . . . Yang, T. T.
574 (2013). Resting-state functional connectivity of subgenual anterior cingulate cortex in
575 depressed adolescents. *Biol Psychiatry*, 74(12), 898-907.
576 doi:10.1016/j.biopsych.2013.05.036
- 577 Cortese, S., Kelly, C., Chabernaud, C., Proal, E., & Di Martino, A., Milham, M. P.,
578 Castellanos, F. X. . (2012). Toward systems neuroscience of ADHD: a meta-analysis
579 of 55 fMRI studies. *American Journal of Psychiatry*, 169(10), 1038-1055.
- 580 Craddock, N., & Owen, M. J. (2010). The Kraepelinian dichotomy - going, going... but still
581 not gone. *Br J Psychiatry*, 196(2), 92-95. doi:10.1192/bjp.bp.109.073429
- 582 Dajani, D. R., Burrows, C. A., Nebel, M. B., Mostofsky, S. H., Gates, K. M., & Uddin, L. Q.
583 (2019). Parsing Heterogeneity in Autism Spectrum Disorder and Attention-
584 Deficit/Hyperactivity Disorder with Individual Connectome Mapping. *Brain Connect*,
585 9(9), 673-691. doi:10.1089/brain.2019.0669
- 586 Di Martino, A., Kelly, C., Grzadzinski, R., Zuo, X. N., Mennes, M., Mairena, M. A., . . .
587 Milham, M. P. (2011). Aberrant striatal functional connectivity in children with
588 autism. *Biol Psychiatry*, 69(9), 847-856. doi:10.1016/j.biopsych.2010.10.029
- 589 Eisenberg, D. P., & Berman, K. F. (2010). Executive function, neural circuitry, and genetic
590 mechanisms in schizophrenia. *Neuropsychopharmacology*, 35(1), 258-277.
591 doi:10.1038/npp.2009.111
- 592 Esteban, O., Birman, D., Schaer, M., Koyejo, O. O., Poldrack, R. A., & Gorgolewski, K. J.
593 (2017). MRIQC: Advancing the automatic prediction of image quality in MRI from
594 unseen sites. *PLoS One*, 12(9), e0184661. doi:10.1371/journal.pone.0184661
- 595 Filippini, N., MacIntosh, B. J., Hough, M. G., Goodwin, G. M., Frisoni, G. B., Smith, S. M., .
596 . . Mackay, C. E. (2009). Distinct patterns of brain activity in young carriers of the
597 APOE- 4 allele. *Proceedings of the National Academy of Sciences*, 106(17), 7209-
598 7214. doi:10.1073/pnas.0811879106
- 599 Francx, W., Oldehinkel, M., Oosterlaan, J., Heslenfeld, D., Hartman, C. A., Hoekstra, P. J., . .
600 . Mennes, M. (2015). The executive control network and symptomatic improvement in
601 attention-deficit/hyperactivity disorder. *Cortex*, 73, 62-72.
602 doi:10.1016/j.cortex.2015.08.012
- 603 Friston, K., Moran, R., & Seth, A. K. (2013). Analysing connectivity with Granger causality
604 and dynamic causal modelling. *Curr Opin Neurobiol*, 23(2), 172-178.
605 doi:10.1016/j.conb.2012.11.010
- 606 Friston, K. J., & Frith, C. D. (1995). Schizophrenia: a disconnection syndrome. *Clin Neurosci*,
607 3(2), 89-97.
- 608 Geiger, M. J., Domschke, K., Ipser, J., Hattingh, C., Baldwin, D. S., Lochner, C., & Stein, D.
609 J. (2016). Altered executive control network resting-state connectivity in social
610 anxiety disorder. *World J Biol Psychiatry*, 17(1), 47-57.
611 doi:10.3109/15622975.2015.1083613
- 612 Griffanti, L., Salimi-Khorshidi, G., Beckmann, C. F., Auerbach, E. J., Douaud, G., Sexton, C.
613 E., . . . Smith, S. M. (2014). ICA-based artefact removal and accelerated fMRI
614 acquisition for improved resting state network imaging. *NeuroImage*, 95, 232-247.
615 doi:10.1016/j.neuroimage.2014.03.034

- 616 Hamm, L. L., Jacobs, R. H., Johnson, M. W., Fitzgerald, D. A., Fitzgerald, K. D.,
617 Langenecker, S. A., . . . Phan K. L. (2014). Aberrant amygdala functional connectivity
618 at rest in pediatric anxiety disorders. *Biology of mood & anxiety disorders*, *4*(1)(15).
- 619 Hengartner, M. P., & Lehmann, S. N. (2017). Why Psychiatric Research Must Abandon
620 Traditional Diagnostic Classification and Adopt a Fully Dimensional Scope: Two
621 Solutions to a Persistent Problem. *Front Psychiatry*, *8*, 101.
622 doi:10.3389/fpsy.2017.00101
- 623 Henry, T. R., Feczko, E., Cordova, M., Earl, E., Williams, S., Nigg, J. T., . . . Gates, K. M.
624 (2019). Comparing directed functional connectivity between groups with confirmatory
625 subgrouping GIMME. *NeuroImage*, *188*, 642-653.
626 doi:10.1016/j.neuroimage.2018.12.040
- 627 Hoff, G. E., Van den Heuvel, M. P., Benders, M. J., Kersbergen, K. J., & De Vries, L. S.
628 (2013). On development of functional brain connectivity in the young brain. *Front*
629 *Hum Neurosci*, *7*, 650. doi:10.3389/fnhum.2013.00650
- 630 Hwang, K., Velanova, K., & Luna, B. (2010). Strengthening of top-down frontal cognitive
631 control networks underlying the development of inhibitory control: a functional
632 magnetic resonance imaging effective connectivity study. *J Neurosci*, *30*(46), 15535-
633 15545. doi:10.1523/JNEUROSCI.2825-10.2010
- 634 Hyvärinen, A. (1999). Fast and robust fixed-point algorithms for independent component
635 analysis. *IEEE Transactions on Neural Networks*, *10*(3), 626–634.
- 636 Insel, T. R. (2010). Rethinking schizophrenia. *Nature*, *468*(7321), 187-193.
637 doi:10.1038/nature09552
- 638 Jalbrzikowski, M., Larsen, B., Hallquist, M. N., Foran, W., Calabro, F., & Luna, B. (2017).
639 Development of White Matter Microstructure and Intrinsic Functional Connectivity
640 Between the Amygdala and Ventromedial Prefrontal Cortex: Associations With
641 Anxiety and Depression. *Biol Psychiatry*, *82*(7), 511-521.
642 doi:10.1016/j.biopsych.2017.01.008
- 643 Jollans, L., & Whelan, R. (2018). Neuromarkers for Mental Disorders: Harnessing Population
644 Neuroscience. *Front Psychiatry*, *9*, 242. doi:10.3389/fpsy.2018.00242
- 645 Kaufmann, T., Alnaes, D., Doan, N. T., Brandt, C. L., Andreassen, O. A., & Westlye, L. T.
646 (2017). Delayed stabilization and individualization in connectome development are
647 related to psychiatric disorders. *Nat Neurosci*, *20*(4), 513-515. doi:10.1038/nn.4511
- 648 Keshavan, M. S., Giedd, J., Lau, J. Y. F., Lewis, D. A., & Paus, T. (2014). Changes in the
649 adolescent brain and the pathophysiology of psychotic disorders. *The Lancet*
650 *Psychiatry*, *1*(7), 549-558. doi:10.1016/s2215-0366(14)00081-9
- 651 Kolskar, K. K., Alnaes, D., Kaufmann, T., Richard, G., Sanders, A. M., Ulrichsen, K. M., . . .
652 Westlye, L. T. (2018). Key Brain Network Nodes Show Differential Cognitive
653 Relevance and Developmental Trajectories during Childhood and Adolescence.
654 *eNeuro*, *5*(4). doi:10.1523/ENEURO.0092-18.2018
- 655 Krueger, R. F., & Bezdjian, S. (2009). Enhancing research and treatment of mental disorders
656 with dimensional concepts: toward DSM-V and ICD-11. . *World Psychiatry*, *8*(1)(3).
- 657 Lee, P. H., Anttila, V., Won, H., Feng, Y.-C. A., Rosenthal, J., Zhu, Z., . . . Smoller, J. W.
658 (2019). Genomic Relationships, Novel Loci, and Pleiotropic Mechanisms across Eight
659 Psychiatric Disorders. *Cell*, *179*(7), 1469-1482.e1411. doi:10.1016/j.cell.2019.11.020
- 660 Li, C., & Tian, L. (2014). Association between resting-state coactivation in the parieto-frontal
661 network and intelligence during late childhood and adolescence. *AJNR Am J*
662 *Neuroradiol*, *35*(6), 1150-1156. doi:10.3174/ajnr.A3850
- 663 Li, C. L., Deng, Y. J., He, Y. H., Zhai, H. C., & Jia, F. C. (2019). The development of brain
664 functional connectivity networks revealed by resting-state functional magnetic

- 665 resonance imaging. *Neural Regen Res*, 14(8), 1419-1429. doi:10.4103/1673-
666 5374.253526
- 667 Li, P., Fan, T. T., Zhao, R. J., Han, Y., Shi, L., Sun, H. Q., . . . Lu, L. (2017). Altered Brain
668 Network Connectivity as a Potential Endophenotype of Schizophrenia. *Sci Rep*, 7(1),
669 5483. doi:10.1038/s41598-017-05774-3
- 670 Li, R., Zhang, J., Wu, X., Wen, X., & Han, B. (2020). Brain-wide resting-state connectivity
671 regulation by the hippocampus and medial prefrontal cortex is associated with fluid
672 intelligence. *Brain Struct Funct*, 225(5), 1587-1600. doi:10.1007/s00429-020-02077-8
- 673 Lund, M. J., Alnaes, D., Schwab, S., van der Meer, D., Andreassen, O. A., Westlye, L. T., &
674 Kaufmann, T. (2020). Differences in directed functional brain connectivity related to
675 age, sex and mental health. *Hum Brain Mapp*. doi:10.1002/hbm.25116
- 676 Mallard, T. T., Linnér, R. K., Okbay, A., Grotzinger, A. D., de Vlaming, R., Meddens, S. F.
677 W., . . . Harden, K. P. (2019). Not just one p: Multivariate GWAS of psychiatric
678 disorders and their cardinal symptoms reveal two dimensions of cross-cutting genetic
679 liabilities. . *bioRxiv*, 603134. doi:10.1101/603134
- 680 Marco, E. J., Hinkley, L. B., Hill, S. S., & Nagarajan, S. S. (2011). Sensory processing in
681 autism: a review of neurophysiologic findings. *Pediatr Res*, 69(5 Pt 2), 48R-54R.
682 doi:10.1203/PDR.0b013e3182130c54
- 683 Muetzel, R. L., Blanken, L. M., Thijssen, S., van der Lugt, A., Jaddoe, V. W., Verhulst, F. C.,
684 . . . White, T. (2016). Resting-state networks in 6-to-10 year old children. *Hum Brain
685 Mapp*, 37(12), 4286-4300. doi:10.1002/hbm.23309
- 686 Pruim, R. H. R., Mennes, M., Buitelaar, J. K., & Beckmann, C. F. (2015). Evaluation of ICA-
687 AROMA and alternative strategies for motion artifact removal in resting state fMRI.
688 *NeuroImage*, 112, 278-287. doi:10.1016/j.neuroimage.2015.02.063
- 689 Pruim, R. H. R., Mennes, M., van Rooij, D., Llera, A., Buitelaar, J. K., & Beckmann, C. F.
690 (2015). ICA-AROMA: A robust ICA-based strategy for removing motion artifacts
691 from fMRI data. *NeuroImage*, 112, 267-277. doi:10.1016/j.neuroimage.2015.02.064
- 692 Rausch, A., Zhang, W., Haak, K. V., Mennes, M., Hermans, E. J., van Oort, E., . . . Groen, W.
693 B. (2016). Altered functional connectivity of the amygdaloid input nuclei in
694 adolescents and young adults with autism spectrum disorder: a resting state fMRI
695 study. *Mol Autism*, 7, 13. doi:10.1186/s13229-015-0060-x
- 696 Riley, J. D., Chen, E. E., Winsell, J., Davis, E. P., Glynn, L. M., Baram, T. Z., . . . Solodkin,
697 A. (2018). Network specialization during adolescence: Hippocampal effective
698 connectivity in boys and girls. *NeuroImage*, 175, 402-412.
699 doi:10.1016/j.neuroimage.2018.04.013
- 700 Salimi-Khorshidi, G., Douaud, G., Beckmann, C. F., Glasser, M. F., Griffanti, L., & Smith, S.
701 M. (2014). Automatic denoising of functional MRI data: combining independent
702 component analysis and hierarchical fusion of classifiers. *NeuroImage*, 90, 449-468.
703 doi:10.1016/j.neuroimage.2013.11.046
- 704 Satterthwaite, T. D., Wolf, D. H., Loughhead, J., Ruparel, K., Elliott, M. A., Hakonarson, H., .
705 . . Gur, R. E. (2012). Impact of in-scanner head motion on multiple measures of
706 functional connectivity: relevance for studies of neurodevelopment in youth.
707 *NeuroImage*, 60(1), 623-632. doi:10.1016/j.neuroimage.2011.12.063
- 708 Schwab, S., Harbord, R., Zerbi, V., Elliott, L., Afyouni, S., Smith, J. Q., . . . Nichols, T. E.
709 (2018). Directed functional connectivity using dynamic graphical models.
710 *NeuroImage*, 175, 340-353. doi:10.1016/j.neuroimage.2018.03.074
- 711 Schweinsburg, A. D., Nagel, B. J., & Tapert, S. F. (2005). fMRI reveals alteration of spatial
712 working memory networks across adolescence. *J Int Neuropsychol Soc*, 11(5), 631-
713 644. doi:10.1017/S1355617705050757

- 714 Shannon, K. E., Sauder, C., Beauchaine, T. P., & Gatzke-Kopp, L. M. (2009). Disrupted
715 Effective Connectivity Between the Medial Frontal Cortex and the Caudate in
716 Adolescent Boys With Externalizing Behavior Disorders. *Criminal Justice and*
717 *Behavior*, 36(11), 1141-1157. doi:10.1177/0093854809342856
- 718 Silk, T., Vance, A., Rinehart, N., Egan, G., O'boyle, M., Bradshaw, J. L., & Cunnington, R.
719 (2005). Fronto-parietal activation in attention-deficit hyperactivity disorder, combined
720 type: functional magnetic resonance imaging study. *The British Journal of Psychiatry*,
721 187(3), 282-283.
- 722 Smeland, O. B., Frei, O., Fan, C.-C., Shadrin, A., Dale, A. M., & Andreassen, O. A. (2019).
723 The emerging pattern of shared polygenic architecture of psychiatric disorders,
724 conceptual and methodological challenges. *Psychiatric Genetics*, 29(5), 152-159.
725 doi:10.1097/ypg.0000000000000234
- 726 Smith, S. M., Fox, P. T., Miller, K. L., Glahn, D. C., Fox, P. M., Mackay, C. E., . . .
727 Beckmann, C. F. (2009). Correspondence of the brain's functional architecture during
728 activation and rest. *Proc Natl Acad Sci U S A*, 106(31), 13040-13045.
729 doi:10.1073/pnas.0905267106
- 730 van den Heuvel, M. P., Stam, C. J., Kahn, R. S., & Hulshoff Pol, H. E. (2009). Efficiency of
731 functional brain networks and intellectual performance. *J Neurosci*, 29(23), 7619-
732 7624. doi:10.1523/JNEUROSCI.1443-09.2009
- 733 Vance, A., Silk, T. J., Casey, M., Rinehart, N. J., Bradshaw, J. L., Bellgrove, M. A., &
734 Cunnington, R. (2007). Right parietal dysfunction in children with attention deficit
735 hyperactivity disorder, combined type: a functional MRI study. *Mol Psychiatry*, 12(9),
736 826-832, 793. doi:10.1038/sj.mp.4001999
- 737 Wechsler, D. (2003). *Wechsler intelligence scale for children--Fourth Edition (WISC-IV)*
- 738 Woolrich, M. W., Ripley, B. D., Brady, M., & Smith, S. M. (2001). Temporal autocorrelation
739 in univariate linear modeling of fMRI data. *NeuroImage*, 14(6), 1370-1386.
740 doi:10.1006/nimg.2001.0931
- 741 Zhao, D., Zheng, S., Yang, L., & Tian, Y. (2017). Causal connectivity abnormalities of
742 regional homogeneity in children with attention deficit hyperactivity disorder: a rest-
743 state fMRI study. *ADMET and DMPK*, 5(4), 242-252. doi:10.5599/admet.5.4.485
- 744 Zhao, Q., Swati, Z. N. K., Metmer, H., Sang, X., & Lu, J. (2019). Investigating executive
745 control network and default mode network dysfunction in major depressive disorder.
746 *Neurosci Lett*, 701, 154-161. doi:10.1016/j.neulet.2019.02.045
747